

Multiobjective Optimization Technique for Mitigating Unbalance and Improving Voltage Considering Higher Penetration of Electric Vehicles and Distributed Generation

Md. Rabiul Islam [✉], *Student Member, IEEE*, Haiyan Lu [✉], *Senior Member, IEEE*,
 Jahangir Hossain [✉], *Senior Member, IEEE*, Md. Rabiul Islam [✉], *Senior Member, IEEE*,
 and Li Li [✉], *Senior Member, IEEE*

Abstract—The increasing penetration of distributed generations (DGs) and electric vehicles (EVs) offers not only several opportunities but also introduces many challenges for the distribution system operators (DSOs) regarding power quality. This article investigates the network performances due to uncoordinated DG and EV distribution. It also considers power quality-related performances such as the neutral current, energy loss, voltage imbalance, and bus voltage as a multiobjective optimization problem. The differential evolution optimization algorithm is employed to solve the multiobjective optimization problem to coordinate EV and DG in a distribution grid. This article proposed a method to coordinate EV and DG distribution. The proposed method allows DSOs to jointly optimize the phase sequence and optimal dispatch of DGs to improve the network's performance. If the network requires further improvement, the EV charging or discharging rate is coordinated for a particular location. The efficacy of the proposed method is tested in an Australian low-voltage distribution grid considering the amount of imbalance due to higher penetration of DG and EV. It is observed that the proposed method reduces voltage unbalance factor by up to 98.24%, neutral current up to 94%, and energy loss by 59.45%, and improve bus voltage by 10.42%.

Index Terms—Compensating neutral current, coordinated/uncoordinated charging, distributed generation (DG) dispatch, electric vehicle (EV), mitigating voltage unbalance.

I. INTRODUCTION

DUE to the increasing pressures of greenhouse gas emission and climate change, electric vehicles (EVs) have been growing as a popular choice for daily transportation. It has been reported in [1] that 12 million EVs have been sold already.

Manuscript received April 24, 2019; revised September 26, 2019 and January 15, 2020; accepted January 15, 2020. Date of publication February 4, 2020; date of current version September 2, 2020. This work was supported by the Australian Government Research Training Program. (*Corresponding author: Md. Rabiul Islam.*)

M. R. Islam, H. Lu, J. Hossain, and L. Li are with the Faculty of Engineering and Information Technology, University of Technology Sydney, Broadway, NSW 2007, Australia (e-mail: mdrabiul.islam-1@student.uts.edu.au; haiyan.lu@uts.edu.au; jahangir.hossain@uts.edu.au; li.li@uts.edu.au).

M. R. Islam is with the Faculty of Engineering and Information Sciences, University of Wollongong, Wollongong, NSW 2522, Australia (e-mail: mrislam@uow.edu.au).

Digital Object Identifier 10.1109/JSYST.2020.2967752

Estimates indicate that world cumulative sales will increase to 200 million by 2030 [1]. On the other hand, more and more distributed generation (DG) sources, e.g., photovoltaic (PV) solar energy and battery energy storage (BES)—are increasingly adding to the distribution grid.

The increasing penetration of DGs and EVs induces the network imbalance in the low voltage (LV) distribution grid which has attracted attention in recent decades [2], [3]. The higher penetration of EV charging loads usually distribute unevenly in a distribution grid [3], causes considerable voltage imbalance, e.g., 3.44 times than balanced scenario was reported in [3]. The uncontrolled DG integration at different penetration levels further increases voltage imbalance [2], [4], transformer overloading and fault currents [5], [6] in an LV distribution grid [2], [4]. The amount of voltage, current [7], power imbalance [8], and energy loss increase when both EV and DG units are integrated in an uncoordinated method. This network imbalance reduces available hosting capacity which leads to reduced uptake of network asset and increased reinforcement cost [9]–[11].

The charging and discharging powers of EVs are coordinated by using the centralized and decentralized control method [12]. In a centralized and decentralized control method, each EV controller regulates the state of charge (SoC) of each EV to achieve the objective (minimize the peak load, energy cost and energy loss, mitigate the uncertainty of renewable energy (RE) based DGs, regulate voltage and frequency) [12]. EV battery SoC was optimized to reduce the load demand in peak time and suitable EV charging time based on the peak demand profile of the network was set using the artificial neural network [13]. To minimize the energy loss of the network and maximize the energy delivered to EV [14], EV charging SoC was optimized using the particle swarm optimization (PSO) algorithm [15]. EV charging or discharging SoC was also optimized to meet the peak demand and minimize the uncertainty of RE-based DGs [16]. The voltage and frequency were regulated by optimizing the EV charging or discharging SoC [17], [18]. However, to the best knowledge of authors, only a few articles have addressed the mitigation of network imbalance in an LV distribution grid.

TABLE I
MAJOR OBJECTIVES CONSIDERED EVCC IN UNBALANCED NETWORK

Ref.	Control approach	Objective			
		Energy loss or utilization	Voltage	VUF	Neutral current
[14]	Centralized	√	×	×	×
[17]	Decentralized	×	√	×	×
[19]	Centralized	×	×	√	×
[22]	Decentralized	√	×	×	×
[23]	Centralized and Decentralized	√	×	×	×
[24]	Decentralized	√	×	×	×
[25]	Centralized and Decentralized	×	√	×	×
[26]	Centralized	√	×	×	×
[27]	Centralized	√	×	×	×
[28]	Decentralized	√	×	×	×
[29]	Centralized	×	√	×	×
Proposed method	Centralized	√	√	√	√

The objective voltage unbalance factor (VUF) was reduced by controlling SoC value of each EV using the PSO algorithm and assuming balanced DGs dispatch [19]. The desired objective was optimized using the metaheuristic optimization approach which shows more efficient performance than seen in simulated annealing, backtracking algorithm, exhaustive search, and greedy algorithm [20]. For coordinating EVs, the metaheuristic optimization approach, i.e., genetic algorithm (GA) and PSO are commonly used [12].

The survey conducted in [18]–[21] indicates that the EV SoC control strategy reduces the comfort level of EV users. Another drawback of the proposed technology is that the network imbalance due to RE-based DGs is not considered in the optimization problem. Further important imbalance indices listed in [2] form the neutral current which is not investigated in an EV penetrated unbalanced distribution grid. The objective function related to EV coordinated control (EVCC) methods is listed in Table I.

To highlight the network imbalance, this article's main contribution is to propose a multiobjective optimization problem to coordinate EVs and DGs jointly in an unbalanced distribution grid. In the multiobjective function, the network imbalance indices (VUF, and the neutral current), the network's voltage, and the energy loss are considered, subject to various network constraints. The differential evolution (DE) optimization algorithm is used to solve the multiobjective problem. The efficacy of the DE optimization algorithm is investigated over commonly metaheuristic optimization approaches. An economical-tariff timeslot is assumed to obtain an optimum solution. This article further offers a proposal for an improved coordinating method not present in the traditional approaches. The proposed method jointly coordinates phases and DGs dispatch of the network by keeping constant EV SoC in the primary control level and optimized SoC of a group of EVs from a sensitive location in the secondary control level to improve the voltage profile, voltage

imbalance, and the neutral current to network standard. The key contributions of this article are as follows:

- 1) proposing a multiobjective optimization problem to mitigate the network imbalance, voltage profile and energy loss of the network;
- 2) proposing an improved control approach which ensures DSOs use the available network capacity efficiently and increases the level of comfort to EV users.

The proposed multiobjective method is expanded upon and the test system is described in Section II. An improved method is proposed in Section III. Results and discussions for uncoordinated and proposed coordinated methods are presented in Section IV, being considered in different network scenarios. Section V concludes the article.

II. PROBLEM FORMULATION AND SYSTEM MODELS

In this section, the mathematical modeling of the devices under consideration including residential loads, EVs, BESs, and PVs are described briefly. A multiobjective optimization problem is formulated to mitigate the network imbalance and voltage profile of a distribution grid.

A. Modeling the Test System and Constraints

The LV distribution network, representing an urban area in Brisbane, Australia [30], is modeled in this article. Each residential load, EV, PV, and BESs are integrated to the distribution network. The distribution network is a three-phase four wire system. A feeder consisting of 13 nodes [31] is considered as test system I in this article which is supplying 88 residential customers, whereas the test system II is assumed of having 44 nodes and 972 residential consumers. The distribution network is connected to the MV network through a two-winding transformer 11/0.4 kV. In this article, the compensation devices such as voltage regulators and shunt capacitors are not considered for both test systems to investigate the efficacy of the proposed method.

The load data for residential consumers were obtained from DSO over a one year of period with average of one hour. For modeling purpose, the power factor of each household is set at 0.96 lagging. The load is modeled as constant active power (P) with power factor 0.96 lagging. The residential loads are considered as single-phase load and distributed among phases in a distribution grid.

To represent 100% EV penetration, it is assumed that each resident owns an EV which is connected to the distribution network. In this article, 100% EV penetration is assumed to investigate the network performance. EV charging profile depends on the battery capacity, EV charger, and the network capacity. The capacity of the test distribution network is increased to support 100% EV penetration. In this article, lithium-ion battery technology is considered and a detailed model is given in [32]. Three types of single-phase EVs were considered and the power consumption depends on the type of EV charger at each timeslot—Level 2 HCS-50 (9.6 kW); Level 2 HCS-60 (11.5 kW); and Level 2 HCS-80 (15.4 kW). Each EV is connected to the distribution grid in either charging or discharging mode. When EVs are not

connected to the distribution grid, they are not in service and are not included in the optimization process. EV owners arrive at home and integrate their EVs to the distribution grid. It is assumed that EV owners and DSOs make agreement to set desired SoC at each timeslot (t) of a day to balance demand-generation of a distribution grid. Each EV acts as a load while charging and continue charging until reaching the final value of SOC. Each EV acts as a dispatched generation source which is discharging until reaching the minimum value of SOC. The voltage and voltage unbalance at each node depend on the rate of EV charging or discharging, location of EV, and EV charger efficiency η .

In this article, EV batteries which are modeled as load act as constant active power with unity power factor at a timeslot (t). EVs dispatched power is modeled as generation source with unity power factor at a timeslot (t) of a day. Each EV is charging or discharging at the desired level of SoC at a timeslot (t). In the optimization process, the SoC value of each EV varies between minimum SoC values SOC_{\min} to maximum SoC value SOC_{\max} as given in (1). NEV represents the number of total EVs. The n represents an EV which belongs to NEV . The t represents each timeslot of a day which belongs to T (24 h). EV charging or discharging SoC value should not be less than the minimum SoC value and must be limited to the maximum SoC value. The charging $P_{EV_{ch}}$ or discharging power $P_{EV_{dch}}$ transfer to the distribution grid depends on the EV charger and distribution grid infrastructures. The EV power consumption or dispatch should be within the limit as given in (2) and (3) at a timeslot (t)

$$SOC(n, t)_{\min} \leq SOC(n, t) \leq SOC(n, t)_{\max} \quad (1)$$

$$P(n, t)_{EV_{dch} \min} \leq P(n, t)_{EV_{dch}} \leq P(n, t)_{EV_{dch} \max} \quad (2)$$

$$P(n, t)_{EV_{ch} \min} \leq P(n, t)_{EV_{ch}} \leq P(n, t)_{EV_{ch} \max} \quad (3)$$

where $n \in NEV$ and $t \in T$.

EVs with different charger ratings are connected among phases (phase-a, phase-b, and phase-c) in a distribution grid. The total power P_t is the lumped sum of three-phase power. The Φ belongs to three-phase (phase-a, phase-b, and phase-c). The degree of imbalance τ due to unequal distribution of EVs among phases is modeled in (4). EV charging loads move from phase A (P_a) and phase C (P_c) to phase B (P_b) with the increasing value of τ . The value of $\tau = 0$ means that EVs are equally distributed among phases and the value of τ gradually increases to 100%

$$\begin{aligned} P_a &= P_a - \tau \\ P_b &= P_b + 2 \times \tau \\ P_c &= P_c - \tau \end{aligned} \quad (4)$$

where $\tau = \%$ of $\frac{P_t}{3}$, $P_t = \sum_{\Phi \in a, b, c} P_{\Phi}$.

For a PV solar power plant, the intermittent characteristics of solar energy plays an important role on the active power output [33]. The PV output power depends on solar irradiance I_{ir} in kW/m^2 . Moreover, the active power output of a PV plant depends on PV solar array efficiency (ε) and the corresponding temperature factor $f(T)$ for ambient temperature (T) [34]. The PV plant produces the direct current (dc) power output P_{PVdc}

as given in the following equation:

$$P_{PVdc} = P_{array} \times \varepsilon \times I_{ir} \times f(T). \quad (5)$$

It is assumed that BESs are integrated with the PV solar plant. In this article, the PV solar and BES are considered as a DG unit. The output dc power of each DG unit is converted to the alternating current (ac) by using the inverter for integrating to the distribution grid. The development of converter technology allows the output power of each DG unit to be controllable. In this article, it is assumed that each household has a DG unit rated from 5 to 20 kW. In the optimization process, the output active power P_{DG} and reactive power Q_{DG} of each DG at node or bus (i) are constrained as shown in (6) and (7) at a timeslot (t) of a day. The node or bus i belongs to the total bus $NBus$ of a distribution grid

$$P(t)_{DG_{\min}}^i \leq P(t)_{DG}^i \leq P(t)_{DG_{\max}}^i \quad (6)$$

$$Q(t)_{DG_{\min}}^i \leq Q(t)_{DG}^i \leq Q(t)_{DG_{\max}}^i \quad (7)$$

where $i \in NBus$ and $t \in T$.

In this article, the 15:00 hr of a summer day is considered as an investigating time slot (t). Our aim is to improve the network performance which does not depend on the EV charging cost [22]. The network performance is investigated in this article by considering residential load profile and EVs at the investigating timeslot. The EV and DG constraints are applied at the investigating time slot (t). In the optimization process, the real time (the investigating time slot) demand of residential and EV charging load, delivered power through EV discharging and dispatched power from each DG (PV plant and BES) unit are considered in this article.

The unbalanced load flow (ULF) model which was proposed in [35] is applied in this article to model the distribution network.

Assuming an arbitrary branch (l, m) in the distribution network, the terminal voltages of the branch are expressed by the Kirchhoff voltage law [36] as given in the following equation:

$$V_l = V_m - Z_{lm} I_{lm} \quad (8)$$

where $V_l = [V_l^a, V_l^b, V_l^c, V_l^n]$, $V_m = [V_m^a, V_m^b, V_m^c, V_m^n]$ is the three-phase voltage at bus l and m . $I_{lm} = [I_{lm}^a, I_{lm}^b, I_{lm}^c, I_{lm}^n]$ is the vector of three-phase current flowing from l to m . Z_{lm} presents impedance which consists of the resistance R_{lm} and reactance X_{lm} as described in [37]. The impedance Z_{lm} is converted to Y_{lm} and the injected current I_l^j at a bus for a given phase j can be calculated from the following equation:

$$I_l^j = \sum_{m=1}^N \sum_{q \in a, b, c} Y_{lm}^{jq} V_m^q. \quad (9)$$

The three-phase power flow problem (10) is given as follows:

$$S_l^j = V_l^j (I_l^j)^* = V_l^j \sum_{m=1}^N \sum_{q \in a, b, c} (Y_{lm}^{jq})^* (V_m^q)^* \quad (10)$$

where S_l^j is the delivered complex power. In this article, the DigSILENT Power Factory software package is able to execute ULF by using the Newton Raphson method described in [38].

To restrain the impact of optimization in the investigating time slot (t), the maximum branch current and the number of lines should remain the same. The total amount of delivered power by DG (PV and BES) and EV discharging power into the network after optimization $P_{DG_optimized}$ will not exceed the total existing (uncoordinated) DG dispatch power $P_{DG_uncoordinated}$ of that network as shown in (11) and (12). The total power consumption due to optimization $P_{load_optimized}$ should be remained same as uncoordinated power consumption $P_{load_uncoordinated}$ shown in (13) and (14)

$$\sum_{i \in NBus} P(t)_{DG_optimized}^i \leq \sum_{i \in NBus} P(t)_{DG_uncoordinated}^i \quad (11)$$

$$\sum_{i \in NBus} Q_{DG_optimized}^i(t) \leq \sum_{i \in NBus} Q_{DG_uncoordinated}^i(t) \quad (12)$$

$$\sum_{i \in NBus} P(t)_{load_optimized}^i = \sum_{i \in NBus} P(t)_{load_uncoordinated}^i \quad (13)$$

$$\sum_{i \in NBus} Q_{load_optimized}^i(t) = \sum_{i \in NBus} Q_{load_uncoordinated}^i(t) \quad (14)$$

$$V(t)_{avg_uncoordinated}^i \leq V(t)_{avg_optimized}^i \quad (15)$$

$$P(t)_{loss_optimized} \leq P(t)_{loss_uncoordinated} \quad (16)$$

where $i \in NBus$ and $t \in T$.

The bus voltage after optimization $V_{avg_optimized}$ must be equal or above the uncoordinated network's bus voltage $V_{avg_uncoordinated}$ as shown in (15) at the investigating timeslot. The total power loss constraint (16) can be defined that the total optimized power loss $P_{loss_optimized}$ should be less than or equal to the uncoordinated network's power loss $P_{loss_uncoordinated}$ at the investigating timeslot (t).

B. Multiobjective Function

The proposed multiobjective function considers the four main objectives as follows.

1) *Voltage Unbalance Factor*: In this article, the most commonly used indicator VUF is employed for analysis to understand the degree of imbalance during power flow computation. VUF is defined as the ratio between negative sequence voltage components V_- and positive sequence voltage components V_+ . For voltage imbalance, the following (17) is used for calculating the VUF. In Australia VUF <2% is the network standard [39], [40]. The objective γ_1 for voltage unbalance factor is as shown in the following equation at a timeslot (t):

$$\gamma_1 = \text{VUF} = \frac{|V(t)_-|^i}{|V(t)_+|^i} \quad (17)$$

where $i \in NBus$ and $t \in T$.

2) *Neutral Current*: The neutral current of an ideal balanced system is zero, whereas neutral current I_n is a summation of three-phase current (I_a, I_b, I_c) at the supporting feeder as

shown in (18). The neutral current can be minimized by minimizing the objective γ_2 as shown in the following equation:

$$I(t)_n = \gamma_2 = I(t)_a + I(t)_b + I(t)_c \quad (18)$$

where $t \in T$.

3) *Bus Voltage*: The bus voltage in an unbalanced distribution grid is defined as the average voltage V_{avg} of phases (phase-a, phase-b, and phase-c) as shown in (19), and the slack bus voltage V_s is 1.05 p.u. Our aim is to increase the average bus voltage at each node by minimizing the deviation between the slack bus voltage and average bus voltage. Equation (20) is expressed the objective function γ_3 to improve the node/bus voltage at a timeslot (t)

$$V(t)_{avg}^i = \frac{\sum_{\Phi \in a,b,c} V(t)_{\Phi}^i}{3} \quad (19)$$

$$\gamma_3 = \sum_{i \in NBus} |V(t)_s - V(t)_{avg}^i| \quad (20)$$

where $i \in NBus$ and $t \in T$.

4) *Energy Loss*: The energy loss is proposed as an objective function γ_4 . The energy loss of the network is a lumped sum of line losses of each branch at a timeslot (t) as shown in (21), where r_{br} , I_{br} are respectively resistance, and current of branch (br) and $Nbranch$ are the total number of branches in the system

$$\gamma_4 = \sum_{br \in Nbranch} r_{br} \times |I_{br}|^2 \quad (21)$$

where $i \in NBus$ and $t \in T$.

Therefore, each objective is combined in the proposed multiobjective (22) with corresponding importance factor $\psi, \zeta, \beta, \kappa$. The higher value of importance factor indicates more improvement on the corresponding objective function. The sum of importance factors must be equal to 1

$$\text{OF}_{\text{proposed}} = \min (\psi \times \gamma_1 + \zeta \times \gamma_2 + \beta \times \gamma_3 + \kappa \times \gamma_4) \quad (22)$$

where $\psi + \zeta + \beta + \kappa = 1$.

The linear scalarization method employed in this article reduces computation burden more than Pareto-based methods [21] for solving the multiobjective optimization problem efficiently. In this article, each individual objective (the neutral current or VUF or bus voltage or energy loss) is not within the same scale. So, it is challenging to choose an appropriate value of weighting factor for solving multiobjective optimization problem. The scaling problem of objectives is obtained by employing ideal and nadir values [18] of individual objectives to convert each objective to the same scale. Each optimization problem (energy loss, voltage imbalance, node voltage, and the neutral current) is solved individually as a single objective function to get nadir and ideal value [41]. In this article, a method which is addressed in [19] is employed for fuzzification of objective functions convert each objective to the same scale [0, 1]. Each individual objective value is converted to fuzzy variable within the same scale using

the following equation:

$$f_k = \begin{cases} 0 & \text{when } f_j \leq 0 \\ f_j & \text{when } 0 < f_j < 1 \\ 1 & \text{when } f_j \geq 1 \end{cases} \quad (23)$$

where $f_j = \frac{\gamma_h - \gamma_h^{\text{nadir}}}{\gamma_h^{\text{ideal}} - \gamma_h^{\text{nadir}}}$ and $h, j, k = 1, 2, 3, 4$.

The value of fuzzy variable f_j for each objective function may not be within the scale [0, 1]. If the value of f_j is above 1, the proposed formula (23) restricts the value of fuzzy member f_k to 1 and if the value of f_j is negative, it replaces by 0 and keeps the same value $f_k = f_j$ if within [0, 1]. In this way, we ensure the fuzzy membership of each objective is kept within the same scale [0, 1]. Therefore, the proposed multiobjective (22) is converted with fuzzy members to the new multiobjective, shown as follows:

$$OF_{\text{proposed}} = \min(\psi \times f_1 + \zeta \times f_2 + \beta \times f_3 + \kappa \times f_4) \quad (24)$$

where $\psi + \zeta + \beta + \kappa = 1$.

The network performances are obtained using the three-phase ULF. The DigSILENT power factory software package executes the ULF by using the Newton Raphson method. The proposed optimization problem is solved using the DE optimization algorithm. This algorithm is described in [31] and is implemented using the DigSILENT power factory package. Both tasks (the ULF and DE optimization) are implemented by using the DigSILENT power factory language capability (DPL) script which is linked to the SCADA server via a text file.

III. PROPOSED METHOD

A centralized control method is proposed here to improve the network performance. The assumptions under which this approach is implemented are that a central controller has access to data, e.g., demand, generation, and network configuration at each timeslot (t) and the DSO has the following features:

- 1) capability to resequence phases dynamically at each node;
- 2) an efficient converter to control output power of DGs;
- 3) an efficient EV charger to control charging or discharging power.

The flowchart shown in Fig. 1 illustrates the logic flow of the proposed method. The input data and required information are imported from the supervisory control and data acquisition (SCADA) network and stored in a linked text file at the SCADA server. Those data are passed to the simulator DigSILENT power factory using the DPL capability at each time slot (t) of a day. The network performance is calculated at the time slot (t). The control criteria include the amount of allowable neutral current (TC), allowable number of nodes (NB_{Volt}) violating the standard bus voltage and allowable number of nodes (NB_{VUF}) having VUF more than standard VUF. The standard bus voltage is 0.95–1.05 p.u. and VUF value is less than 2% according to Australian network standard [39], [40]. If the control criteria are violated, the DE optimization algorithm will be executed by using the DPL capability. The best fitness of the objective (24) is achieved by considering constraints (6)–(7) and (11)–(16). The constraints (13) and (14) keep the EV charging or discharging

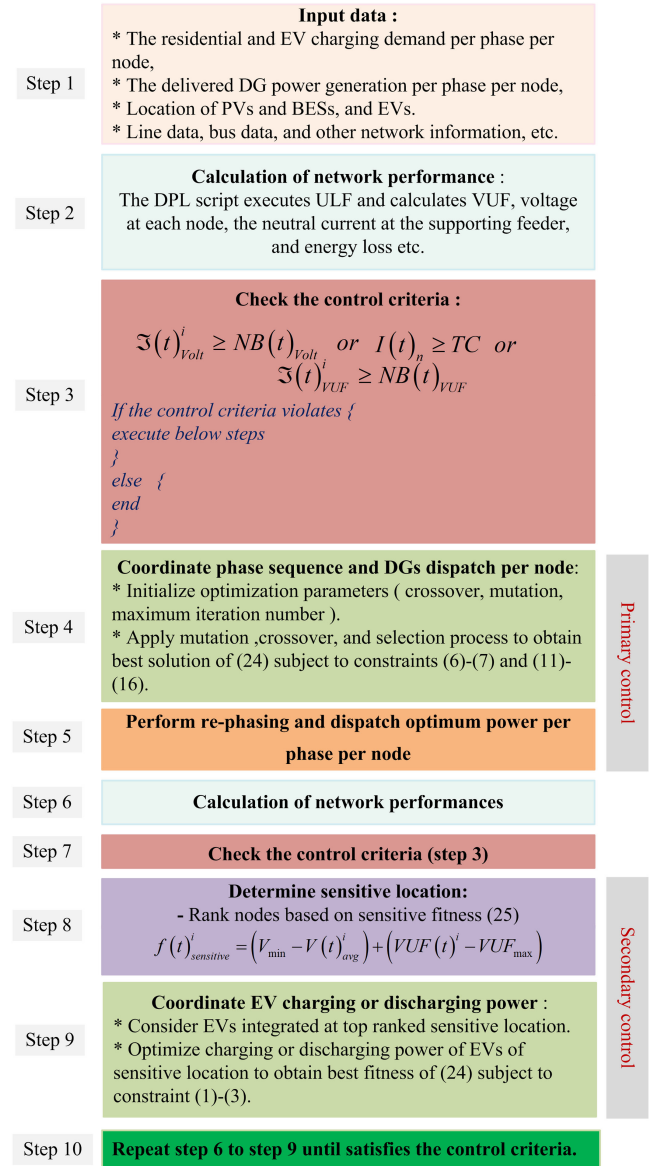


Fig. 1. Flowchart of the proposed method.

power unchanged. The proposed method recommends an optimal phase sequence (coordinate EVs with desired SoC) at the respective node and optimum DGs dispatch among phases per node. In this article, the phase sequence {A, B, C} is presented as 0, whereas the sequence of phases {B, C, A} is given as P and {C, A, B} is as N. The optimal coordination of phase sequence and optimum dispatch of DGs is expressed as the primary control approach.

The optimum EVs and DGs configuration is exported to the SCADA server by using the DPL script. The network is reconfigured by using the SCADA framework. The network performance is obtained by executing the ULF. If the control criteria are still not achieved, the proposed method performs a secondary control approach, where the sensitive location is obtained based on the sensitive fitness (25). The sensitive fitness of each node or bus is the summation of bus voltage and VUF deviation. The bus voltage deviation is the deviation between

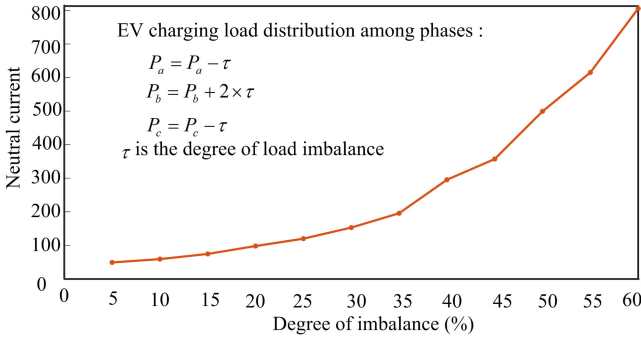


Fig. 2. Neutral current with increased the degree of imbalance.

standard minimum voltage (V_{\min}) and the bus voltage of a node at the investigating time (t). The VUF deviation is defined as the deviation between standard maximum VUF (VUF_{\max}) and the VUF of a node at the investigating time (t). For this approach, $V_{\min} = 0.95$ p.u. and $VUF_{\max} = 2\%$ is considered.

$$f(t)_{\text{sensitive}}^i = \left(V_{\min} - V(t)_{\text{avg}}^i \right) + \left(VUF(t)^i - VUF_{\max} \right). \quad (25)$$

The node having higher positive value based on sensitive fitness (25) is considered as a sensitive node or location. The charging or discharging power of EVs connected at the sensitive node is optimized to improve the network performance. If satisfactory network performance is still not achieved, a group of EVs charging or discharging power of another sensitive location will optimize. The proposed method repeats EV coordination procedures until it satisfies the control criteria.

The proposed method allows participation of both DSOs and EVs to improve the network performance. The DSO resequences phases and coordinates DGs dispatch to reduce participation of EV users at the primary control. If the network performance is still below the control criteria, EVs charging or discharging rate is optimized in a particular location at the secondary control. In this way, the proposed control method maximizes the level of comfort of an EV user.

IV. RESULTS AND DISCUSSION

In order to evaluate the effectiveness of the proposed method, we implemented it in both test systems. The distribution system in the test systems is considered as a three-phase unbalanced grid by uneven distribution of EVs. The impact of uncoordinated EVs distribution among phases is investigated by varying the degree of imbalance τ according to (4) subject to load flow convergence.

Fig. 2 shows that the neutral current is increasing with increasing the degree of imbalance from 0% to 60%. The load flow does not converge beyond the degree of imbalance 60%. This article evaluates the performance of the proposed method considering the following three scenarios by varying the degree of imbalance τ .

- 1) Scenario I: Uncoordinated method.
- 2) Scenario II: Proposed coordinated method considering the degree of imbalance $\tau = 30\%$.
- 3) Scenario III: Proposed coordinated method considering the degree of imbalance $\tau = 40\%$.

TABLE II
OPTIMAL REPHASING AND POWER DISPATCH PER NODE (TEST SYSTEM I)

Scenario	Re-phasing (Bus no.)	Generation power dispatch (kW)/ (Bus no.)	
		$P(t)_{DG}^i = \sum_{\Phi \in a,b,c} P(t)_{DG}^i$	
Scenario I (Uncoordinated)	-	180(B611),	140(B632),
		22(B633),	23(B634),
		145(B645),	41(B646),
		130(B652),	40(B671),
		171(B675),	39(B680),
		10(B684),	28(B692).
Scenario II (Proposed coordinated)	B632 (N), B634 (N), B645 (P), B646 (P), B671 (N), B692 (P).	80(B611),	234(B632),
		19(B633),	33(B634),
		205(B645),	22(B646),
		130(B652),	54(B671),
		126(B675),	44(B680),
		09(B684),	14(B692).

A. Scenario I: Uncoordinated Method

In scenario I, EVs are connected in an uncoordinated EV charging method. The degree of imbalance τ due to EV charging is 30%. Each DG unit is also dispatching power to the distribution network. The impact of uncoordinated method is investigated by executing the ULF considering τ is 30%. In the test system I, the VUF value is above 2% (from 2.85% to 9.50%) at all the buses, and the bus voltage is below 0.95 p.u (0.85–0.92 p.u) at 10 buses out of 13 buses. The bus voltage is below 0.95 p.u at 19 buses out of 44 buses in the test system II. The obtained results show a significant amount of energy loss (190.64 kW) and the neutral current (49.58 A) at the supporting feeder of the test system I. The neutral current at the test system II is 195.49 A and energy loss is 1359.427 kW.

B. Scenario II: Proposed Coordinated Method Considering the Degree of Imbalance $\tau = 30\%$.

The DE optimization algorithm is carried out to solve the optimization problem (24) considering scheduled generation. The proposed coordinated method is applied to both the test system I and II considering τ is 30%.

The weighting factor is selected based on the importance of corresponding network performance. The single objective (VUF) optimization shows that it also reduces the bus voltage [19], the neutral current [42], and the energy loss of a distribution network [42]. The optimization of the neutral current and VUF as a multiobjective also increases bus voltage [31]. Our aim has more importance on reducing the network imbalance VUF, and the neutral current. For this reason, we assign higher importance factor for the network imbalance (neutral current $\psi = 0.35$, VUF $\zeta = 0.35$), voltage $\beta = 0.2$, and energy loss $\kappa = 0.1$ to solve the proposed multiobjective (24) in this article.

The proposed method solves the multiobjective optimization problem (24) subject to the network constraint (11)–(16). The proposed method coordinates the phase sequence, and DG power dispatch per phase per node as shown in Tables II and III. The rephasing nodes are listed with the type of phase sequence (P for

TABLE III
OPTIMAL REPHASING AND POWER DISPATCH PER NODE (TEST SYSTEM II)

Scenario	Re-phasing (Bus no.)	Generation power dispatch (kW) / (Bus no.)		
		$P(t)_{DG}^i = \sum_{\Phi_{a,b,c}} P(t)_{DG}^j$		
Scenario I (Uncoordinated)	-	906 (B02), 687(B03), 1401(B04), 45(B05), 49(B06), 427(B07), 55(B08), 100(B09), 10(B10), 250(B11), 26(B12), 357(B13), 344(B14), 180(B15), 53(B16), 670(B17), 432(B18), 11(B19), 197(B20), 95(B21), 551(B22), 100(B23), 200(B24), 200(B25), 567(B26), 428(B27), 129(B28), 150(B29), 200(B30), 800(B31), 200(B32), 350(B33), 200(B34), 618(B35), 200(B36), 63(B37), 3.0(B38), 150(B39), 210(B40), 150(B41), 200(B42), 200(B43), 100(B44).		
	Scenario II (Proposed coordinated)	B02(N), 1006 (B02), 752 (B03), 1768 (B04), 48 (B05), 23 (B06), 455 (B07), 63 (B08), 6 (B09), 12 (B10), 218 (B11), 25 (B12), 454 (B13), 359 (B14), 181 (B15), 38 (B16), 783 (B17), 501 (B18), 13 (B19), 237 (B20), 112 (B21), 695 (B22), 62 (B23), 57 (B24), 40 (B25), 698 (B26), 468 (B27), 156 (B28), 2 (B29), 4 (B30), 987 (B31), 7 (B32), 331 (B33), B35(P), 73 (B34), 801 (B35), 211 (B36), 59 (B37), 2 (B38), 0.0 (B39), 245 (B40), 28 (B41), 270 (B42), 14 (B43), 1.0 (B44).		

positive and N for negative phase sequence) and optimal power dispatch per node or bus. The proposed method is not recommending all nodes to participate in rephasing which reduces the rephasing execution time. The optimum power delivered to each node is controlled by regulating the dispatch of DG unit. The EV discharging power is kept constant at the investing timeslot (t).

The improvement of VUF and bus voltage using the proposed coordinated method compared to the uncoordinated method is as shown in Figs. 3 and 4 of the test system I. Figs. 3 and 4 show that the proposed coordinated method minimizes the VUF value below 2% at all buses and reduces VUF value up to 98.24% at node #bus 645 compared to the uncoordinated method. The bus voltage is improved above 0.95 p.u. at all the buses and improves the bus voltage up to 9.44% compared to the uncoordinated method. The proposed method reduces the neutral current from 49.58 to 3.13 A and the energy loss from 190.64 to 77.31 kW. The performance of the proposed method is compared with the uncoordinated method of the test system II is given in Figs. 5 and 6. The efficacy of the proposed method is summarized in Tables IV and V.

From Tables IV and V, it is observed that the maximum VUF value is 9.50% (B 611) in the uncoordinated method. The proposed method reduces the maximum VUF value to 1.91% (B 611), which is even less than the minimum VUF value 2.85% (B 692) obtained in the uncoordinated method in test system I. In test system II, the proposed coordinated method reduces

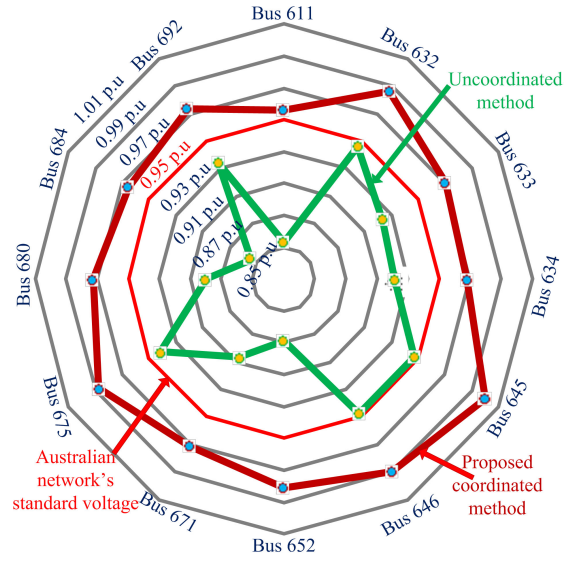


Fig. 3. Voltage at different node (test system I).

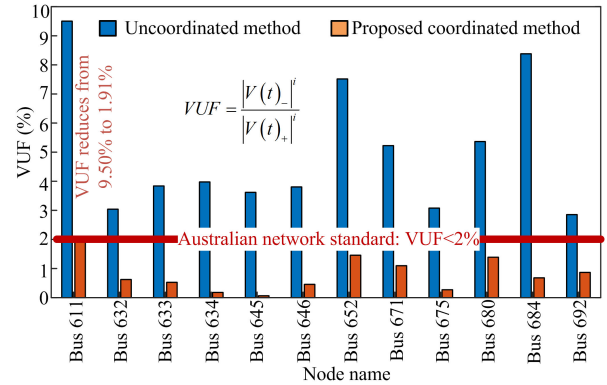


Fig. 4. Voltage unbalance factor at different node (test system I).

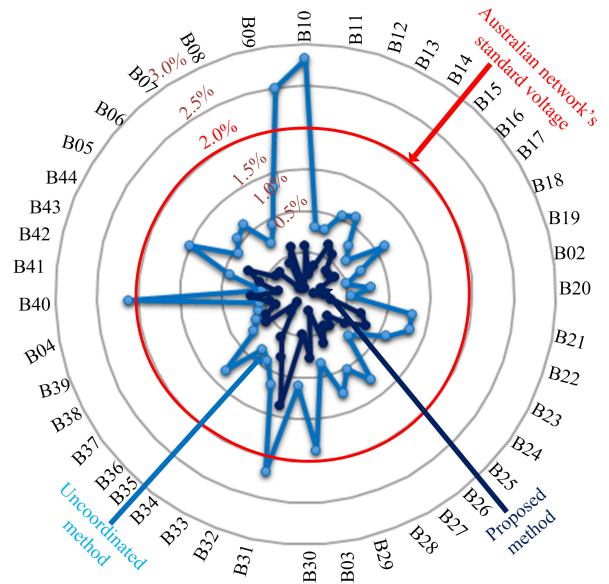


Fig. 5. Voltage unbalance factor at different node (test system II).

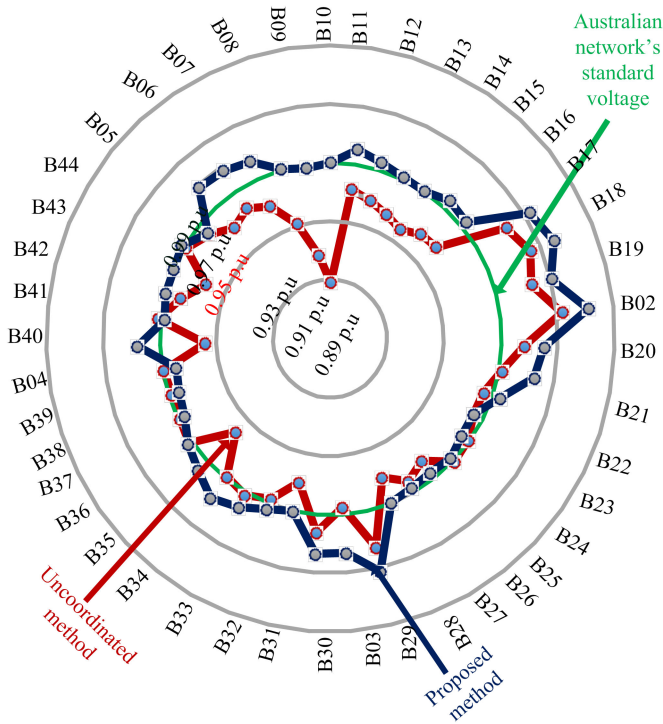


Fig. 6. Voltage at different node (test system II).

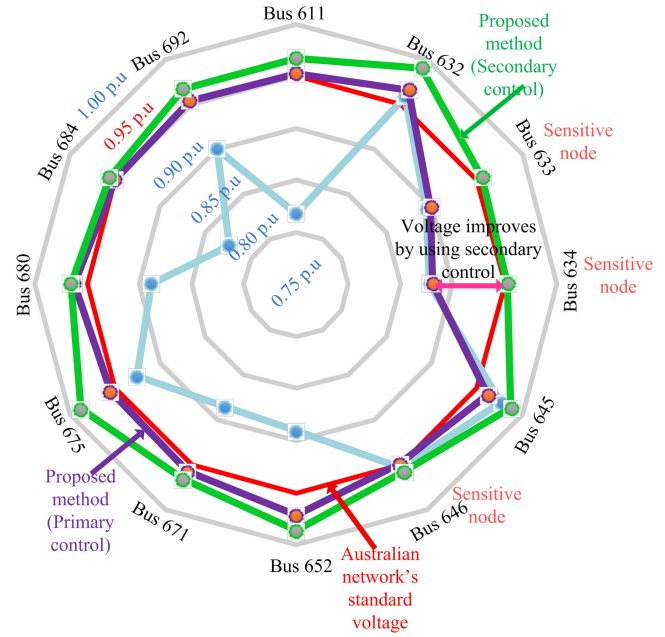
 TABLE IV
 NETWORK PERFORMANCE OF THE TEST SYSTEM I

Network Performance Index	Scenario I (Uncoordinated)	Scenario II (Proposed method)
VUF (max)	9.50% (B611)	1.91% (B611)
VUF (min)	2.85% (B692)	0.06% (B645)
Bus voltage (max)	0.95 p.u (B632)	1.00 p.u (B645)
Bus voltage (min)	0.87 p.u (B684)	0.96 p.u (B645)
Neutral current	49.58 A	3.13 A
Power loss (kW)	190.64	77.31

 TABLE V
 NETWORK PERFORMANCE OF THE TEST SYSTEM II

Network Performance Index	Scenario I (Uncoordinated)	Scenario II (Proposed method)
VUF (max)	2.83% (B10)	1.37% (B31)
VUF (min)	0.51% (B19)	0.07% (B09)
Bus voltage (max)	0.97 p.u (B18)	0.99 p.u (B18)
Bus voltage (min)	0.91 p.u (B10)	0.95 p.u (B10)
Neutral current	195.49 A	39.59 A
Power loss (kW)	1359.427	1253.539

the maximum VUF value from 2.83% to 1.37%. The minimum value of bus voltage is 0.87 p.u. at the test system I and 0.91 p.u. at the test system II. The proposed coordinated method improves bus voltage, where the minimum value of bus voltage is 0.95 p.u for both test systems. The control criteria are achieved by using the proposed control method with primary control approach and the proposed method does not require to implement secondary control approach. Therefore, the proposed coordinated method


 Fig. 7. Voltage at different node ($\tau = 40\%$).

improves the network performance without reducing EV charging power or importing power from the external grid.

C. Scenario III: Proposed Coordinated Method Considering the Degree of Imbalance $\tau = 40\%$.

In this scenario, it is assumed that the power delivered to the distribution grid, the residential and EV charging demands remain same as in scenario I. The degree of imbalance τ is considered 40% in this scenario III. The network performance is executed by using the ULF. The increased degree of imbalance increases the VUF up to 12.02% (B 611) and decreases the bus voltage to 0.82 p.u. (B 611) in the test system I.

The coordinated method proposed is applied to the test system I. Its performance is presented by two control approaches: primary control and secondary control. The method is compared with the uncoordinated method as given in Figs. 7 and 8. From Figs. 7 and 8, it is observed that the primary control approach (optimum rephasing and DG dispatch) increases bus voltage and reduces the voltage imbalance. But the bus voltage is still below the control criteria (0.95 p.u.) at the #bus 632, #bus 633, and #bus 634 and the VUF value is still below the control criteria at nodes #bus 611, #bus 632, # bus 633, #bus 634, #bus 645, # bus 646.

The proposed method recommends to implement the secondary control approach to satisfy the control criteria. The sensitive location (node in a distribution grid) is selected based on the value of sensitive fitness (25). The worst node #bus 634 is selected as a sensitive location. The EV charging or discharging power of bus 634 is optimized for solving (24) subject to individual EV constraint (1)–(3). In this article, the control criteria are achieved after optimizing EV SoC of sensitive locations # bus 634, # bus 633, and #bus 646. Figs. 7 and 8 show

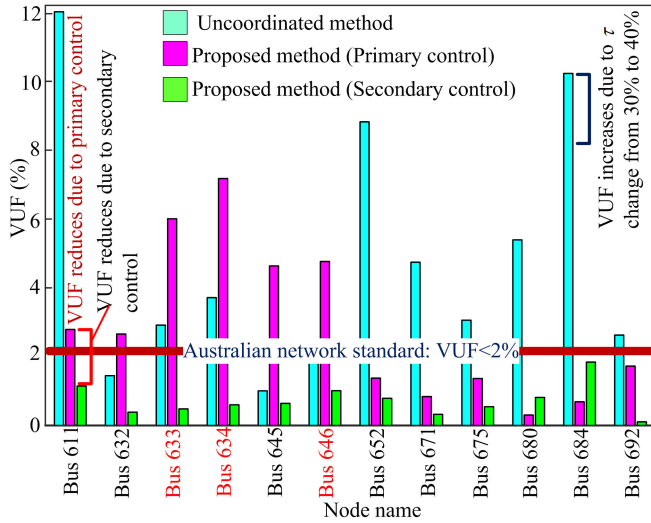


Fig. 8. Voltage unbalance factor at different node ($\tau = 40\%$).

that the bus voltage above 0.95 p.u and VUF is less than 2% at all the node.

The increasing degree of imbalance τ increases the voltage imbalance and the neutral current, and decreases bus voltage in a distribution grid. The constraint of keeping constant demand per node in the rephasing method is the limitation to balancing the distribution grid completely. The unbalanced distribution grid requires more power supply [43] but the total output power generation of the network remains constant (13), (14). Though the primary control approach, considering both constraints, cannot achieve the control criteria, the proposed method ensures comfortability for EV users. In the secondary control approach, 32 EVs out of 88 EVs charging or discharging power is controlled. Therefore, the proposed method offers comfortability to the rest of 56 EV users in scenario III, whereas all EV users in scenario II. This method therefore benefits EV users more than conventional methods discussed in [19].

In this article, the DE optimization algorithm is used to solve the multiobjective optimization problem (24). Our aim is to investigate the efficacy of the DE optimization algorithm by comparing with commonly used optimization algorithms, e.g., GA and PSO to solve EVCC problem [12]. The control parameters (e.g., crossover, mutation, acceleration constants, etc.) of GA, PSO, and DE are initialized. The optimum value of control parameters is obtained when the best fitness is achieved. The optimum crossover probability is 0.77 and mutation probability is 0.15 for GA, whereas the crossover rate is 0.88 and mutation factor (F) is 0.18 for the DE algorithm. The optimum acceleration coefficients $c1 = 0.25$, $c2 = 0.31$ and inertia weight $= 0.8$ are the values applied in the PSO algorithm. The GA, PSO, and DE algorithms are implemented by considering 10 000 evaluations and optimum parameter values to the test system II by using the proposed method.

Fig. 9 shows the efficacy of optimization algorithms for minimizing the fitness with respect to the number of iteration. The fitness value is zero after 153 iterations using the DE optimization algorithm. The DE optimization algorithm requires fewer

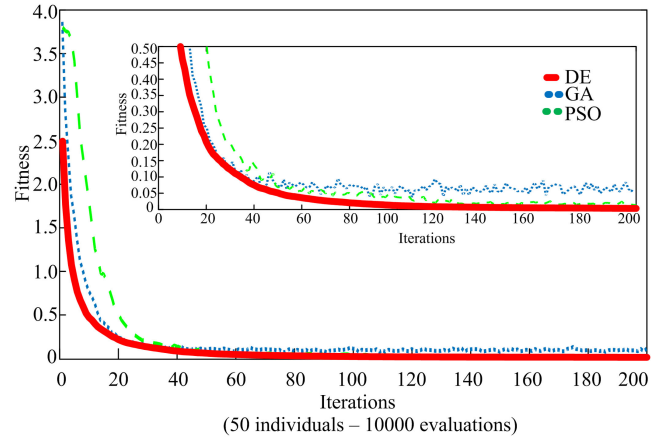


Fig. 9. Performance of GA, PSO, and DE algorithms (proposed method).

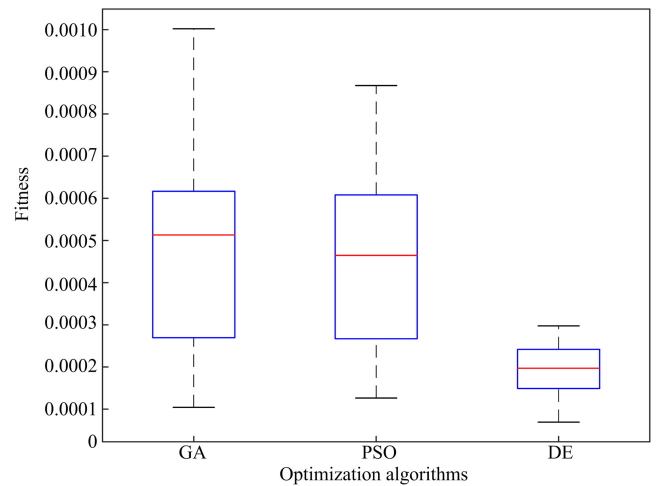


Fig. 10. Statistical performance of GA, PSO, and DE algorithms (proposed method).

TABLE VI
NETWORK PERFORMANCE OF GA, PSO, AND DE ALGORITHM

Network Performance Index	GA	PSO	DE
VUF (max)	1.91% (B10)	1.30% (B09)	1.37% (B31)
Bus voltage (min)	0.93 p.u(B10)	0.93 p.u(B10)	0.95 p.u(B10)

iterations for minimizing the fitness value compared with GA and PSO. The statistical analysis results are presented through a box plot in Fig. 10. This (see Fig. 10) shows that all statistical indicators have reduced to a point for the DE algorithm, meaning higher homogeneity around the median over GA and PSO. Table VI shows that the DE algorithm improves the network performance more than GA and PSO. From, Figs. 9 and 10, and Table VI, it can be concluded that the DE optimization algorithm shows faster convergence speed and improved network performance over GA and PSO.

V. CONCLUSION

The proposed method is used to solve the multiobjective optimization problem, subject to network constraint. The efficacy of the proposed method is evaluated, considering the following three scenarios:

- 1) uncoordinated method;
- 2) coordinated method considering 30% network imbalance;
- 3) coordinated method considering 40% network imbalance in this article.

The uncoordinated method increases the VUF value up to 9.50%, and the bus voltage decrease to 0.87 p.u., due to uncoordinated EV and DG distribution. The proposed method is applied to the test distribution grid, considering the scheduled generation. The proposed method shows improvement of the network performance (bus voltage above 0.95 p.u. and VUF less than 2% for all buses) and allows DSOs to resequence phases and for optimum dispatch of DGs per-phase-per-node of a distribution grid. In scenario II, the proposed method does not require control of EV charging or discharging power. The joint optimization approach of the proposed method increases the level of comfort of the EV user because it does not change the charging or discharging rate of each EV. The proposed method recommends managing the SoC of a group of EVs in a location where the joint optimization approach does not improve the network performance to the desired level, as discussed in scenario III. The multiobjective optimization problem is hereby solved by using the DE optimization algorithm. This algorithm shows not only greater homogeneity and computational superiority but also improves the network performance over the more commonly used optimization algorithms GA and PSO. Therefore, this article recommends the optimizing of phase sequence and DG dispatch at the primary control approach, combined with controlled EV SoC at the corresponding secondary control approach. The method proposed in this article is general and applicable to any LV unbalanced distribution grid.

ACKNOWLEDGMENT

The authors would like to thank ENERGEX for providing the LV network model for research.

REFERENCES

- [1] I.E. Agency, Paris, France, "Global EV outlook," Dec. 2017.
- [2] M. R. Islam, H. Lu, M. J. Hossain, and L. Li, "Mitigating unbalance using distributed network reconfiguration techniques in distributed power generation grids with services for electric vehicles: A review," *J. Cleaner Prod.*, vol. 239, pp. 910–932, Dec. 2019.
- [3] T. Klayklung and S. Dechanupaprittha, "Impact analysis on voltage unbalance of EVs charging on a low voltage distribution system," in *Proc. Int. Elect. Eng. Congr.*, Mar. 2014, pp. 1–4.
- [4] F. J. Ruiz-Rodriguez, J. C. Hernández, and F. Jurado, "Voltage unbalance assessment in secondary radial distribution networks with single-phase photovoltaic systems," *Int. J. Elect. Power Energy Syst.*, vol. 64, pp. 646–654, Jan. 2015.
- [5] K. Balamurugan, D. Srinivasan, and T. Reindl, "Impact of distributed generation on power distribution systems," *Energy Procedia*, vol. 25, pp. 93–100, Jan. 2012.
- [6] P. Juanuwattanukul and M. A. S. Masoum, "Increasing distributed generation penetration in multiphase distribution networks considering grid losses, maximum loading factor and bus voltage limits," *IET Gener., Transmiss. Distrib.*, vol. 6, no. 12, pp. 1262–1271, Dec. 2012.
- [7] F. M. Uriarte and R. E. Hebner, "Residential smart grids: Before and after the appearance of PVs and EVs," in *Proc. IEEE Int. Conf. Smart Grid Commun.*, Nov. 2014, pp. 578–583.
- [8] F. Möller, J. Meyer, and M. Radauer, "Impact of a high penetration of electric vehicles and photovoltaic inverters on power quality in an urban residential grid part i-unbalance," in *Proc. Int. Conf. Renewable Energies Power Quality*, May 2016, pp. 817–812.
- [9] M. K. Gray and W. G. Morsi, "Economic assessment of phase reconfiguration to mitigate the unbalance due to plug-in electric vehicles charging," *Elect. Power Syst. Res.*, vol. 140, pp. 329–336, Nov. 2016.
- [10] K. Ma, R. Li, and F. Li, "Quantification of additional asset reinforcement cost from 3-phase imbalance," *IEEE Trans. Power Syst.*, vol. 31, no. 4, pp. 2885–2891, Oct. 2016.
- [11] M. Sadeghi and M. Kalantar, "The analysis of the effects of clean technologies from economic point of view," *J. Cleaner Prod.*, vol. 102, pp. 394–407, Sep. 2015.
- [12] M. Amjad, A. Ahmad, M. H. Rehmani, and T. Umer, "A review of EVs charging: from the perspective of energy optimization, optimization approaches, and charging techniques," *Transportation Res. D, Transport. Environ.*, vol. 62, pp. 386–417, Jul. 2018.
- [13] K. Mahmud, S. Morsalin, M. J. Hossain, and G. E. Town, "Domestic peak-load management including vehicle-to-grid and battery storage unit using an artificial neural network," in *Proc. IEEE Int. Conf. Ind. Technol.*, Mar. 2017, pp. 586–591.
- [14] P. Richardson, D. Flynn, and A. Keane, "Optimal charging of electric vehicles in low-voltage distribution systems," *IEEE Trans. Power Syst.*, vol. 27, no. 1, pp. 268–279, Feb. 2012.
- [15] M. Esmaili and A. Goldoust, "Multi-objective optimal charging of plug-in electric vehicles in unbalanced distribution networks," *Int. J. Elect. Power Energy Syst.*, vol. 73, pp. 644–652, Dec. 2015.
- [16] T. N. Le, S. Al-Rubaye, H. Liang, and B. J. Choi, "Dynamic charging and discharging for electric vehicles in microgrids," in *Proc. IEEE Int. Conf. Commun. Workshop*, Jun. 2015, pp. 2018–2022.
- [17] J. E. Cardona, J. C. López, and M. J. Rider, "Decentralized electric vehicles charging coordination using only local voltage magnitude measurements," *Elect. Power Syst. Res.*, vol. 161, pp. 139–151, Aug. 2018.
- [18] J. Quirós-Tortós, L. F. Ochoa, S. W. Alnaser, and T. Butler, "Control of EV charging points for thermal and voltage management of LV networks," *IEEE Trans. Power Syst.*, vol. 31, no. 4, pp. 3028–3039, 2016.
- [19] H. F. Farahani, "Improving voltage unbalance of low-voltage distribution networks using plug-in electric vehicles," *J. Cleaner Prod.*, vol. 239, pp. 336–346, Apr. 2017.
- [20] K. Wang, S. Skiena, and T. G. Robertazzi, "Phase balancing algorithms," *Elect. Power Syst. Res.*, vol. 96, pp. 218–224, Mar. 2013.
- [21] S. Shao, M. Pipattanasomporn, and S. Rahman, "Grid integration of electric vehicles and demand response with customer choice," *IEEE Trans. Smart Grid*, vol. 3, no. 1, pp. 543–550, Mar. 2012.
- [22] M. Esmaili and A. Goldoust, "Multi-objective optimal charging of plug-in electric vehicles in unbalanced distribution networks," *Int. J. Elect. Power Energy Syst.*, vol. 73, pp. 644–652, Dec. 2015.
- [23] P. Richardson, D. Flynn, and A. Keane, "Local versus centralized charging strategies for electric vehicles in low voltage distribution systems," *IEEE Trans. Smart Grid*, vol. 3, no. 2, pp. 1020–1028, Jun. 2012.
- [24] M. Esmaili and M. Rajabi, "Optimal charging of plug-in electric vehicles observing power grid constraints," *IET Gener., Transmiss. Distrib.*, vol. 8, no. 4, pp. 583–590, Apr. 2014.
- [25] J. d. Hoog *et al.*, "Electric vehicle charging and grid constraints: Comparing distributed and centralized approaches," in *Proc. IEEE Power Energy Soc. General Meeting*, Jul. 2013, pp. 1–5.
- [26] F. Milano and O. Hersent, "Optimal load management with inclusion of electric vehicles and distributed energy resources," *IEEE Trans. Smart Grid*, vol. 5, no. 2, pp. 662–672, Mar. 2014.
- [27] N. B. Arias, J. F. Franco, M. Lavorato, and R. Romero, "Metaheuristic optimization algorithms for the optimal coordination of plug-in electric vehicle charging in distribution systems with distributed generation," *Elect. Power Syst. Res.*, vol. 142, pp. 351–361, Jan. 2017.
- [28] S. Weckx, R. D'Hulst, B. Claessens, and J. Driesensam, "Multiagent charging of electric vehicles respecting distribution transformer loading and voltage limits," *IEEE Trans. Smart Grid*, vol. 5, no. 6, pp. 2857–2867, Nov. 2014.
- [29] J. F. Franco, M. J. Rider, and R. Romero, "A mixed-integer linear programming model for the electric vehicle charging coordination problem in unbalanced electrical distribution systems," *IEEE Trans. Smart Grid*, vol. 6, no. 5, pp. 2200–2210, Sep. 2015.

- [30] F. H. M. Rafi, M. J. Hossain, M. S. Rahman, and J. Lu, "Implementation of independent improved neutral current controller using four leg PV-VSI," in *Proc. Australasia Univ. Power Eng. Conf.*, Sep. 2016, pp. 1–6.
- [31] M. R. Islam, H. H. Lu, M. J. Hossain, and L. Li, "A comparison of performance of GA, PSO and differential evolution algorithms for dynamic phase reconfiguration technology of a smart grid," in *Proc. IEEE Congr. Evol. Comput.*, Jun. 2019, pp. 858–865.
- [32] L. Zhang, L. Wang, G. Hinds, C. Lyu, J. Zheng, and J. Li, "Multi-objective optimization of lithium-ion battery model using genetic algorithm approach," *J. Power Sources*, vol. 270, pp. 367–378, Dec. 2014.
- [33] M. R. Islam and H. I. Walldi, "Ramp rate analysis of roof-top PV on distribution grids for large cities in Australia," in *Proc. 4th Int. Conf. Develop. Renewable Energy Technol.*, Jan. 2016, pp. 1–5.
- [34] M. K. Gray and W. G. Morsi, "On the impact of single-phase plug-in electric vehicles charging and rooftop solar photovoltaic on distribution transformer aging," *Elect. Power Syst. Res.*, vol. 148, pp. 202–209, Jul. 2017.
- [35] B. Sereeter, K. Vuik, C. Witteveen, and R. Tiako, "Newton power flow methods for unbalanced three-phase distribution networks," *Energies*, vol. 10, pp. 10–21, Oct. 2017.
- [36] H. F. Zhai, M. Yang, B. Chen, and N. Kang, "Dynamic reconfiguration of three-phase unbalanced distribution networks," *Int. J. Elect. Power Energy Syst.*, vol. 99, pp. 1–10, Jul. 2018.
- [37] W. H. Kersting, *Distribution System Modeling and Analysis*. Boca Raton, FL, USA: CRC Press, Sep. 2012.
- [38] D. G., Stuttgart, Germany, "DigSILENT powerfactory software package," 2018. [Online]. Available: <https://www.digsilent.de>
- [39] Australian National Electricity Rules, Version 117, 2019. [Online]. Available: <https://www.aemc.gov.au>. Accessed on: Jan. 11 2019.
- [40] IEEE Recommended Practice for Monitoring Electric Power Quality, vol. IEEE Standard 1159-1995, 1995. [Online]. Available: <https://doi.org/10.1109/ieeestd.1995.79050>. Accessed on: Jan. 14, 2019.
- [41] K. Miettinen, *Nonlinear Multiobjective Optimization*. New York, NY, US: Springer, 1998.
- [42] S. H. Soltani, M. Rashidinejad, and A. Abdollahi, "Dynamic phase balancing in the smart distribution networks," *Int. J. Elect. Power Energy Syst.*, vol. 93, pp. 374–383, Dec. 2017.
- [43] A. Hintz, U. R. Prasanna, and K. Rajashekara, "Comparative study of the three-phase grid-connected inverter sharing unbalanced three-phase and/or single-phase systems," *IEEE Trans. Ind. Appl.*, vol. 52, no. 6, pp. 5156–5164, Nov./Dec. 2016.



Md. Rabiul Islam (Student Member, IEEE) received the M.Sc. degree in renewable energy from the University of Oldenburg, Oldenburg, Germany, in 2015, and the B.Sc. degree in electrical and electronic engineering from the Rajshahi University of Engineering & Technology, Rajshahi, Bangladesh, in 2007. He is currently working toward the Ph.D. degree with the Centre for Artificial Intelligence, FEIT, University of Technology Sydney (UTS), Sydney, NSW, Australia.

He was a Lecturer with the Pabna University of Science and Technology (PUST) in 2011 and promoted

to Assistant Professor in 2014. He was a Research Associate with Overspeed GmbH & Company KG, Oldenburg, Germany, in 2014. His research interests include heuristic optimization techniques, renewable energy, electric vehicle integration, prediction of solar energy, and smart and flexible electricity grid.

Mr. Islam was the recipient of the prestigious German government scholarship (DAAD) in 2013 and UTS President's Award in 2017.



Haiyan (Helen) Lu (Senior Member, IEEE) received the bachelor's and master's degrees from the Harbin Institute of Technology, Harbin, China, in 1985 and 1988, respectively, and the Ph.D. degree from the University of Technology Sydney (UTS), Sydney, NSW, Australia, in 2002.

She is currently an Associate Professor with the School of Computer Science, Faculty of Engineering and Information Technology, and a core member of the Decision Systems and e-Service Intelligence Research Laboratory, Centre for Artificial Intelligence, UTS. She has authored or coauthored 3 book chapters, 68 refereed journal papers, and 82 refereed international and national conference papers. Her main research interests are heuristic optimization techniques, forecasting and prediction of time series, ontology-based knowledge representation, recommendation systems and causal relationship, and inference and reasoning in data streams.



M. Jahangir Hossain (Senior Member, IEEE) received the B.Sc. and M.Sc. Eng. degrees from the Rajshahi University of Engineering & Technology, Rajshahi, Bangladesh, and the Ph.D. degree from the University of New South Wales, Sydney, NSW, Australia.

He is currently an Associate Professor with the School of Electrical and Data Engineering, UTS, Sydney, NSW, Australia. Before joining there, he was an Associate Professor with Macquarie University, Australia, and a Senior Lecturer and a Lecturer with Griffith University, Australia. His research interests include renewable energy integration and stabilization, microgrids and smart grids, and energy storage systems.



Md. Rabiul Islam (Senior Member, IEEE) received the Ph.D. degree in electrical engineering from the University of Technology Sydney, Sydney, NSW, Australia, in 2014.

He was a Lecturer with the Rajshahi University of Engineering & Technology, Rajshahi, Bangladesh, in 2005, and promoted to a Full Professor in 2017. In early 2018, he joined the School of Electrical, Computer, and Telecommunications Engineering, University of Wollongong, Wollongong, Australia. He has authored 140 papers in international journals and conference proceedings. He has written or edited four technical books published by Springer. His research interests include power electronic converters, renewable energy technologies, electrical machines, and smart grid.



Li Li (Senior Member, IEEE) received the B.S. degree from the Huazhong University of Science and Technology, Wuhan, China, in 1996, the M.S. degree from Tsinghua University, Beijing, China, in 1999, and the Ph.D. degree from the University of California, Oakland, CA, USA, in 2005.

He is currently an Associate Professor with the School of Electrical and Data Engineering, University of Technology Sydney, Sydney, NSW, Australia. Before joining here, he was a Research Associate with the University of New South Wales, Australia, and Victoria Research Laboratory, University of Melbourne, Australia. His research interests include control theory and power system control.